Evaluating the Accuracy of BMP280 and BME280 Sensors for Sea Level in a Coastal Environment: A Field Study at Tanjung Siambang Pier

Hollanda Arief Kusuma[1]*, Yuliani[1], Tonny Suhendra[1], Dhanushka Devendra[2], Dwi Eny Djoko Setyono[3]

[1]*Department of Electrical Engineering, Universitas Maritim Raja Ali Haji*
Jl. Politeknik Senggarang, Tanjungpinang, Indonesia
[2]*Department of Electrical Engineering, Institute of Oceanology Polish Academy of Sciences*
Powstańców Warszawy 55, 81-712 Sopot, P.O. Box 148, Poland
[3]*Research Center for Food Technology and Processing, National Research and Innovation Agency*
Jl. Jogja, Wonosari KM. 31,5. Gading IV. Gading. Kec. Playen, Gunung Kidul, Indonesia
Email: hollandakusuma@umrah.ac.id

Abstract

Monitoring sea level is important for assessing climate change impacts, coastal management, and predicting hazards. Accurate measurements of air pressure is essential for precise sea level monitoring through pressure-to-altitude conversion. Additionally, understanding tidal patterns and their dominant components is crucial for comprehensive sea level analysis. This research aimed to investigate the accuracy of BMP280 and BME280 sensors in measuring air pressure and altitude to monitor sea level. Comparing air pressure data from the BMP280, BME280, and BMKG sensors showed that the BMP280 sensor had a higher accuracy than the BME280 sensor. Linear regression was used to decrease the error value. After calibration, BME280 and BMP280 did not differ with the BMKG sensor using one-way ANOVA and Tukey test. A field test was also conducted to assess the ability of the BMP280 sensor to measure sea level height from air pressure conversion. It was found that the BMP280 sensor could not provide an accurate sea level height value with an R^2 value of 0.00931. A Fourier analysis was used to investigate the tidal pattern in Tanjung Siambang using six constituents, symbols S1, O2, M2, S2, S4, and S6, with periods of 24, 12.91, 12.42, 12, 6, and 4 h. It revealed that the dominant components were M2 and S2, caused by the moon's and the earth's gravitational pull. This study highlights the limitations of the BMP280 sensor in providing accurate sea level height measurements and the importance of the M2 and S2 tidal components in determining sea tides in Tanjung Siambang.

Keywords: *BMP280, BME280, Sea Level, Air Pressure, Fourier Analysis*

Introduction

Tides are the regular rise and fall of sea levels caused by the gravitational pull of the Moon and the Sun on Earth. The knowledge of tides is important for coastal communities, as it affects many aspects of life, such as shipping, port construction, and offshore development. Understanding tides is crucial for ensuring ships' safe and efficient operation and for planning the construction of ports, sea highways, and other infrastructure in coastal areas (Qiang, *et al.*, 2018; Wang *et al.*, 2018). Additionally, the information is useful for planning underwater activities such as planting pipelines or cables and underwater communication (Missa *et al.*, 2018; Guo *et al.*, 2020; Bello and Zeadally, 2022).

There are several methods in use for measuring tides, including ultrasonic sensors such as HC-SR04, traditional tide gauges, acoustic systems, and radar technology (Asaad *et al.*, 2018; Haq *et al.*, 2021; Intergovernmental Oceanographic Commission, 2006; Missa *et al.*, 2018). For example, data obtained can be inaccurate due to problems such as parallax errors, interference during measurement, and the passage of other objects while data is being collected (Towler and Williams, 2010). Additionally, traditional tide gauges are prone to issues such as rusting, which can negatively impact the accuracy of the measurements (Fadly and Dewi, 2019).

Air pressure, or the force exerted on a surface, is affected by the elevation above sea level, with higher elevations experiencing lower air pressure (Yulkifli *et al.*, 2014). Using barometric sensor to measure altitude is a common approach (Bolanakis *et al.*, 2015; Albaladejo-Perez *et al.*, 2017; Kumar and Tanwar, 2020), as it allows for the elimination of errors caused by changes in atmospheric pressure. By comparing the pressure readings from the two sensors, it is possible to accurately determine the height of the sea surface and, thus, the tide level. This

*) Corresponding author

https://ejournal.undip.ac.id/index.php/ijms
DOI: 10.14710/ik.ijms.28.2.189-202
Received : 01-02-2023
Accepted : 26-05-2023

approach is often used in tide gauges and other sea level measurement systems (Richter *et al*., 2016; Bolanakis, 2017).

Through the measurement of air pressure variations at sea level, valuable information about the ebb and flow of seawater, or tides, can be obtained. In this study, an innovative design is proposed, utilizing a Bosch pressure sensor capable of measuring air pressure, humidity, and temperature. These sensors are employed to acquire tidal data and identify different types of tides.

Materials and Methods

The research was conducted over ten months, from March 2021 to December 2021. The instrument design was developed at the Laboratory of the Faculty of Engineering, Universitas Maritim Raja Ali Haji. The field test was carried out at Tanjung Siambang, Dompak Island, Riau Islands, to evaluate the performance of the designed tool in real-world conditions (Figure 1).

Design system

The instrument for measuring tides is designed using several key components, including Bosch pressure sensors (BMP280 and BME280) to measure air pressure and temperature, Arduino Mega Pro 2560 as a microcontroller, RTC DS3231 as a timer, and a Micro SD Card Module for data storage (Figure 2). This design allows for accurate and reliable measurement of tide levels by utilizing the Bosch pressure sensors and the microcontroller to process and record the data, and the RTC DS3231 to provide a real-time clock for timing the measurements. The Micro SD Card Module allows for storage of the data for further analysis and documentation.

Sensor calibration

Calibration is a process used to determine the accuracy of measurement results by comparing them to actual data (Tirtasari, 2017). The barometric pressure sensor must be calibrated at several pressures (Dickow and Feiertag, 2014). In this study, calibration was conducted by comparing the sensor results with the calibrator (Vaisala sensor) at the BMKG Station Raja Haji Fisabilillah Tanjungpinang Airport. This error value helps ensure that the instrument provides accurate and reliable measurements of tide levels. The measurement error was calculated using the following equation:

$$Error = \left| \frac{(calibrator\ data - sensor\ data)}{calibrator\ data} \right| \times 100\% \quad (1)$$

After calibration, the accuracy of the measurement results was assessed using field data and the Root Mean Square Error (RMSE) method. RMSE is a commonly used measure of the difference

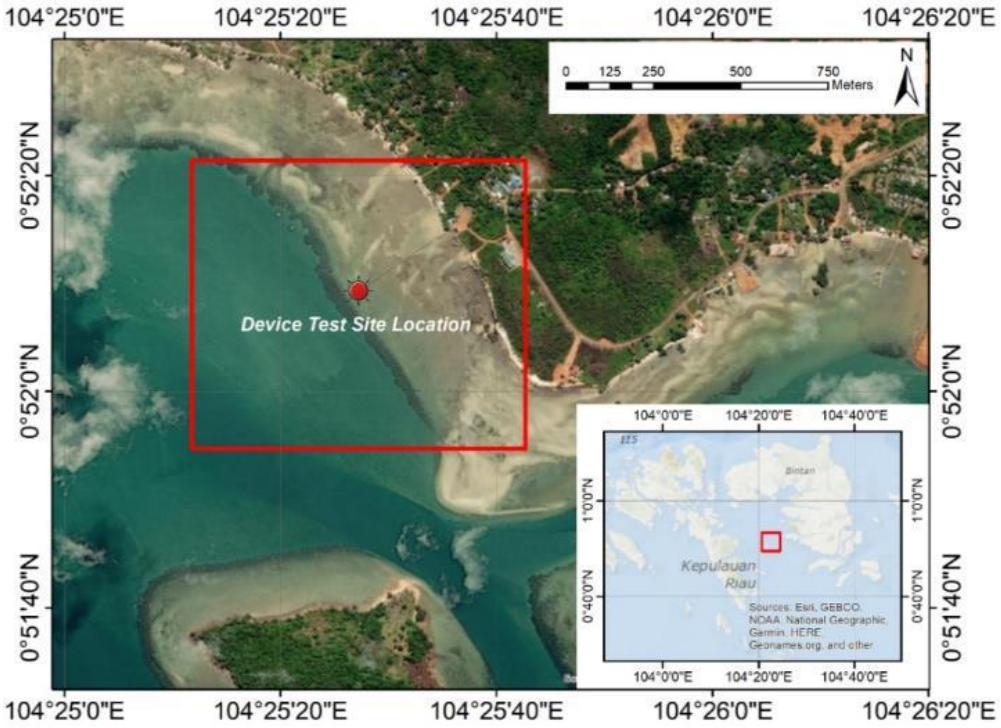

Figure 1. Device testing location at Tanjung Siambang

between predicted and actual values, and it is calculated by taking the square root of the average of the squared differences between the predicted and actual values. The smaller the RMSE value, the better the forecast results (Haq and Ni, 2019). The RMSE value helps to determine the instrument's accuracy and ability to predict tide levels. Calculating RMSE is in the following equation where "n" is the number of data points.

$$\mathrm{RMSE} = \sqrt{\frac{\sum_{i=1}^{n} (\text{predicted value-actual value})^2}{n}} \quad (2)$$

To ensure that BMP280 and BME280 sensor values did not differ from the BMKG sensor, the data were analyzed using one-way ANOVA. The ANOVA determines any statistically significant differences between the sensor's means of air pressure data (Hossain *et al.*, 2020). The level of confidence used is 95% (α=0.05). This analysis of variance requires treatment and replication data. The treatment used in this study is BMP280, BME280, and Vaisala. The replication data uses air pressure data taken every 1 minute from each sensor.

The null hypothesis (H0) is rejected if the F-test value for the mean or average value surpasses the critical value in the F-table. This indicates compelling evidence that at least one treatment differs from another. To assess differences between the means of all possible pairs, the Tukey test is conducted for paired comparisons using a studentized range distribution. The yardstick for this test determines whether a significant difference exists between a pair of treatment means, utilizing the quantity ω (Mendenhall *et al.*, 2013).

$$\omega = q_{\alpha}(k, df)\left(\frac{s}{\sqrt{n_t}}\right) \quad (3)$$

Note: k= Number of treatments; s^2= Mean Square Error; df= Degree of freedom for s^2; nt= Common sample size; qk, df= Tabulated value from Percentage Points of the Studentized Range

Air pressure to altitude conversion

The data obtained from the Bosch pressure sensor in this study was converted to an altitude reading using the barometric pressure formula (Xia *et al.*, 2015). The barometric pressure formula relates the water level, air pressure, air density, and the Earth's gravity as described by the following equation:

$$h = \frac{R.T0}{\mathrm{g.M}} . \ln\frac{P}{P0} \quad (4)$$

Note: P= Pressure (Pascal); P0= Initial Pressure (101325 Pascal); g= Gravity Acceleration (9,80665 $m.s^{-2}$); T0= Temperature (288.15 Kelvin); R= Constant gas (8.31432 $Nm\ mol^{-1}K^{-1}$); M= Molar Mass (0.00289644 $m.s^{-2}$); h= Altitude/height (m)

This equation considers the relationship between pressure, the density of air, and the Earth's gravity to calculate the altitude above sea level. The instrument can provide accurate information on the tide levels by converting the pressure readings to altitude readings.

Tidal analysis

The pressure data obtained from the Bosch pressure sensor was analyzed using Fourier analysis to determine the tidal constituents or components. *Fourier analysis* transforms time-domain data into frequency-domain data (Irtawaty, 2019; Nugent, 2019). Tidal constituents are the main components of the tide, each having an amplitude, period or frequency, and phase (Dina *et al.*, 2019; Rudiastuti *et al.*, 2019). The Fourier analysis is used to identify these constituents, which are used to explain the patterns of the tides and can be used to predict future tide levels. In addition, the results of the Fourier analysis can be used to determine the amplitude of each constituent, which can be used to create a tidal prediction model (Kusuma *et al.*, 2021).

Result and Discussion

Design and construction of the instrument

Component integration begins with the PCB (Printed Circuit Board) design, which is carried out to make the electronic circuit paths neater and reduce the use of jumper wires. After the schematic has been completed, PCB fabrication is then performed. Then, after PCB fabrication, the components are mounted on the PCB. There are two sections of the PCB, the upper part of which is mounted with the BME280 sensor, the BMP280 sensor, and the Micro SD Card Module, while the lower part of the PCB is mounted with the Arduino Mega Pro 2560 and the DS3231 RTC module.

After the components are mounted on the PCB, the next step is to program the Arduino Mega Pro 2560 microcontroller. The programming is done using the Arduino IDE software, where the program code is written in C++. The program code is responsible for reading data from the sensors, storing data on the Micro SD Card, and displaying data on the LCD screen. The program code also includes a module for data logging, which stores data in the Micro SD Card in a specific format for later analysis. The flowchart of this instrument can be seen in Figure 3.

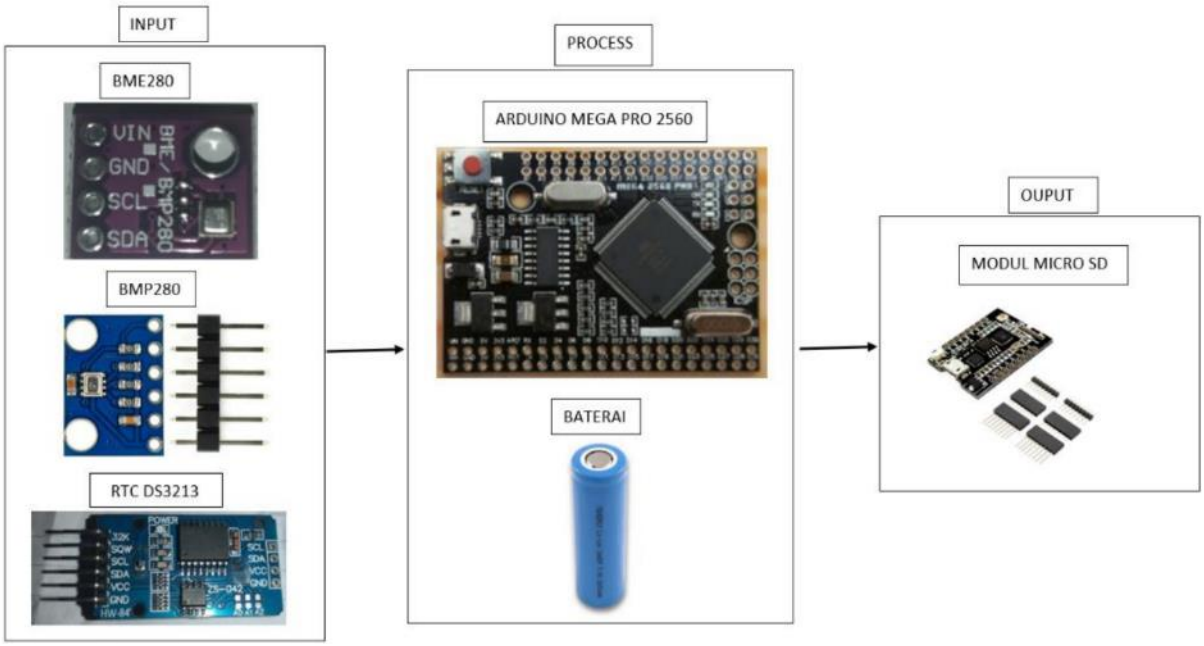

Figure 2. Device system components diagram

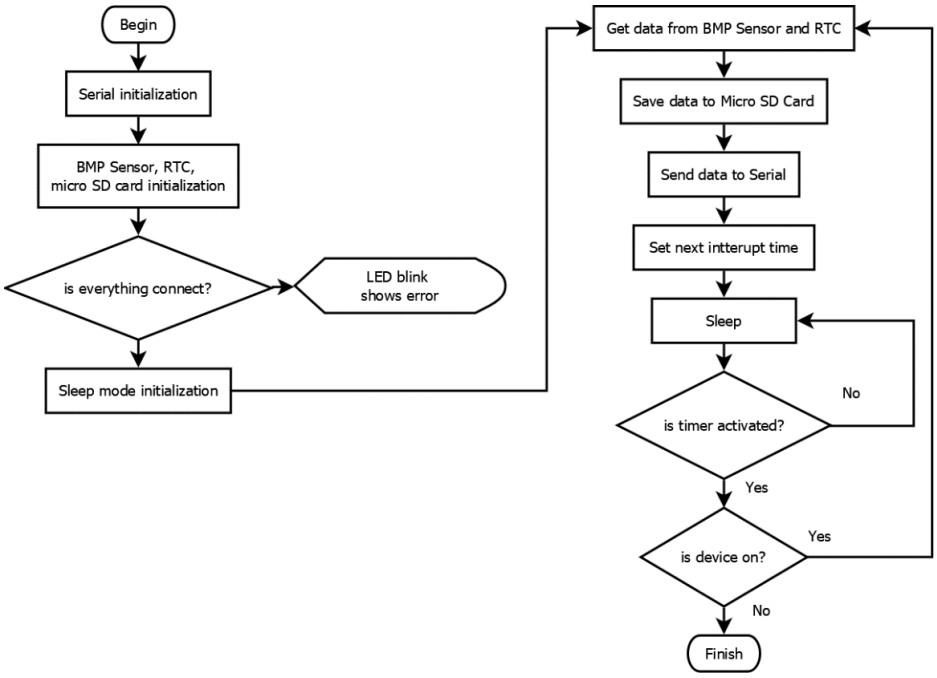

Figure 3. Instrument firmware flowchart

Calibration and testing of the system

This study performed sensor calibration by placing the device at the BMKG (Indonesian Meteorological, Climatological, and Geophysical Agency) for 24 h. Air pressure data were collected every minute and compared with data from the BMP280, BME280, and BMKG sensors. The program for this calibration can be found in this project GitHub (https://tinyurl.com/4sjbnna2). The results of this comparison are shown in Figure 4. From the comparison, it was found that the BMP280 sensor measurements were closer to the BMKG measurements than the BME280 sensor

measurements. Linear regression analysis was then performed on the data, and the results of this analysis are shown in Figures 5 and 6.

The coefficients of determination for the BMP280 sensor were found to be 0.9934, and the BME280 sensor was found to be 0.9946. The accuracy of the measurements was also evaluated using the RMSE (Root Mean Square Error) metric. The RMSE for the BMP280 sensor was found to be 0.16 hPa, and for the BME280 sensor, it was found to be 2.25 hPa. Based on these results, the BMP280 sensor is more accurate than the BME280 sensor.

After calibrating the sensor, the comparison is made between the calibrated sensor and the BMKG sensor results (Figure 7). The program code for this observation, utilizing BMP280 and BME280, is available in the following repository (https://tinyurl.com/ybx2fv9h). Descriptive statistics can be found in Table 1. To visualize the data, a box plot is employed to illustrate the minimum, average, and maximum values of each sensor. (Figure 8.). The raw and calibrated sensor data can be seen in Appendix I.

The calibration results were analyzed using One-Way ANOVA to see the difference between raw BMP280 and BME280, calibrated BMP280 and BME280, and the BMKG sensor. Based on one-way ANOVA analysis, the F-test exceeds the critical value (F-crit). Thus, sufficient evidence indicates that at least one of the sensors differs from the others. Therefore, Tukey test is used to determine which of the sensors differs from the others. The mean values

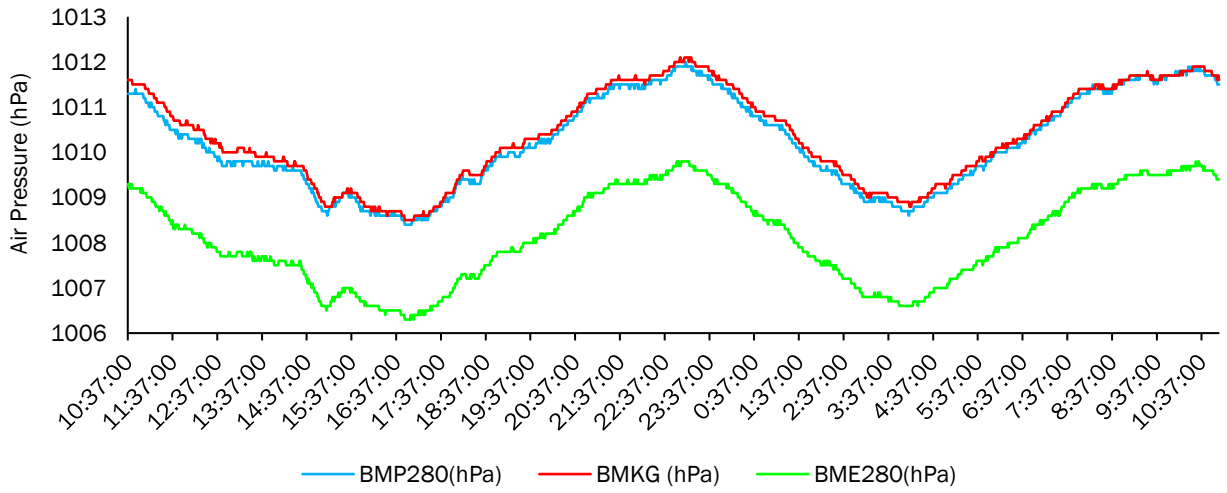

Figure 4. BMP280, BME280, and BMKG sensor measurement results

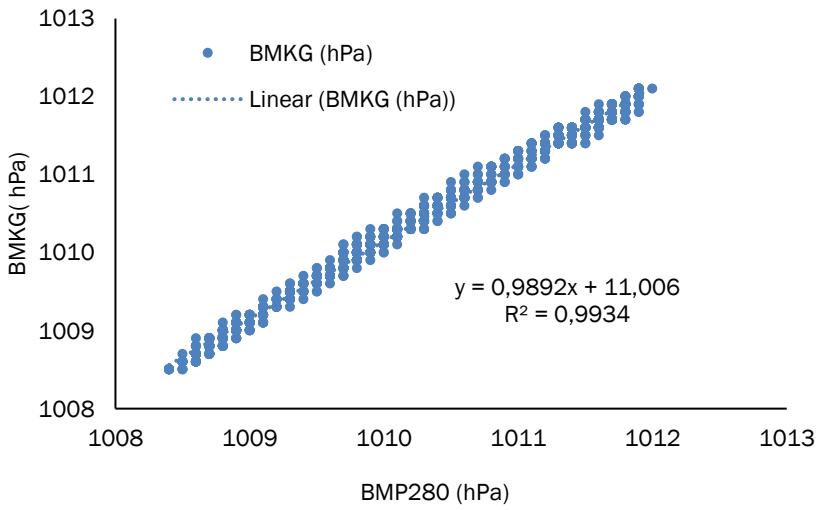

Figure 5. BMP280 linear regression based on calibration data

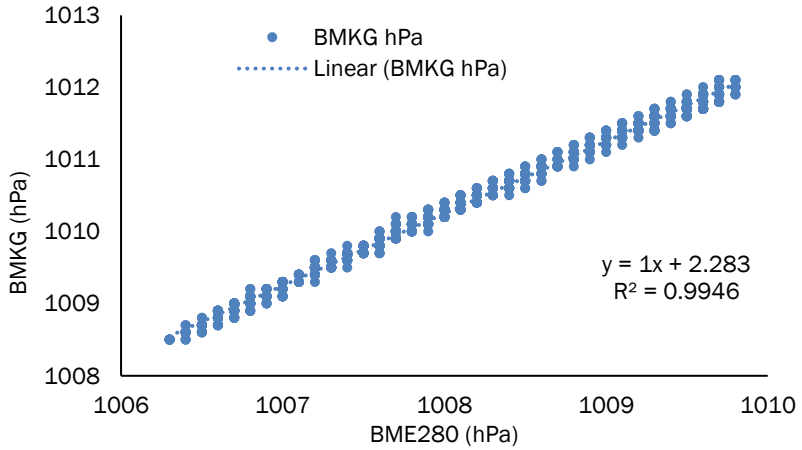

Figure 6. BME280 linear regression based on calibration data

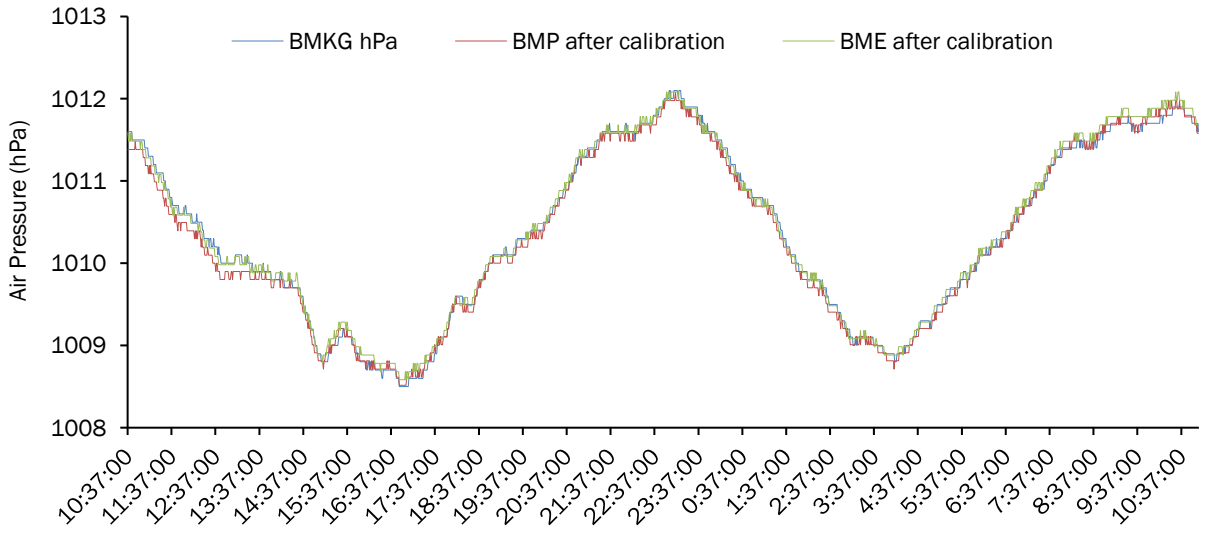

Figure 7. Air Pressure Data comparison between BMP280, BME280, and BMKG after calibration

Table 1. Descriptive statistics between BMP280, BME280, and BMKG sensors

Statistic Parameter	*BMP280 before calibration (hPa)*	*BME280 before calibration (hPa)*	*BMKG (hPa)*	*BMP after calibration (hPa)*	*BME after calibration (hPa)*
Mean	1010.2247	1008.1143	1010.3653	1010.3202	1010.3973
Standard Deviation	1.0481	1.0375	1.0403	1.0368	1.0375
Minimum	1008.4000	1006.3000	1008.5000	1008.5153	1008.5830
Maximum	1012.0000	1009.8000	1012.1000	1012.0764	1012.0830

of each sensor are sorted from lowest to highest, and the differences are assessed against the omega value of 0.09. The matrix presented in Table 2 indicates that the calibrated BMP280 and BME sensors do not exhibit significant differences from the BMKG sensor. Hence, calibration is mandatory for every sensor.

An energy consumption test was conducted to determine the device's power requirements. The test was conducted using a Voltage-Current (VC) Meter (Figuer 9) and was run for one hour. This device consumes an average power of 42.94 mW, an average current of 10.79 mA, and an average voltage of 3,98 V from the 18650 batteries parallel. With a

2200 mAh battery, the device can operate for 203 hours or eight days.

Field test

The field test was conducted by placing two devices, one on a buoy (Figure 10.a) and the other on a wharf (Figure 10.b) at the Tanjung Siambang Pier, starting from 7:35 am on November 12, 2021, until 6:00 am on November 13, 2021. Data were collected every minute for 24 hours. The collected data was then analyzed to compare the two locations' air pressure readings and sea level measurements.

Air pressure to altitude conversion

The results of converting air pressure to altitude were analyzed (Figure 11) and compared to measurements taken using a measuring stick. The data was recorded every 30 min (Figure 12). Figure 11 shows the results of converting air pressure to altitude, while Figure 12 compares these results to measurements taken with a measuring stick. The comparison shows that the sea level height measurements obtained from the BMP280 sensor significantly differ from those taken with the measuring stick. A linear regression analysis with an

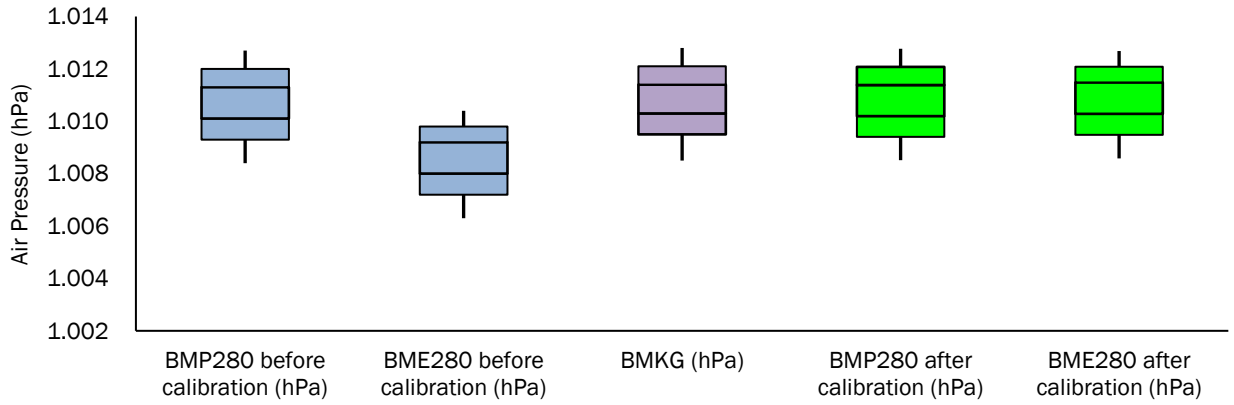

Figure 8. The box plot comparison between BMP280, BME280, and BMKG before and after calibration

Table 2. Matrix Comparison matrix between BMP280, BME280 and BMKG in hPa

	BME280	BMP280	BMP after calibration	BMKG	BME after calibration
BME280	0	2.11	2.21	2.25	2.28
BMP280		0	0.09	0.14	0.17
BMP after calibration			0	0.05	0.07
BMKG				0	0.03
BME after calibration					0

Figure 9. Power measurement using voltage-current meter

(a) (b)

Figure 10. Device 1 on buoy (a) and Device 2 on wharf

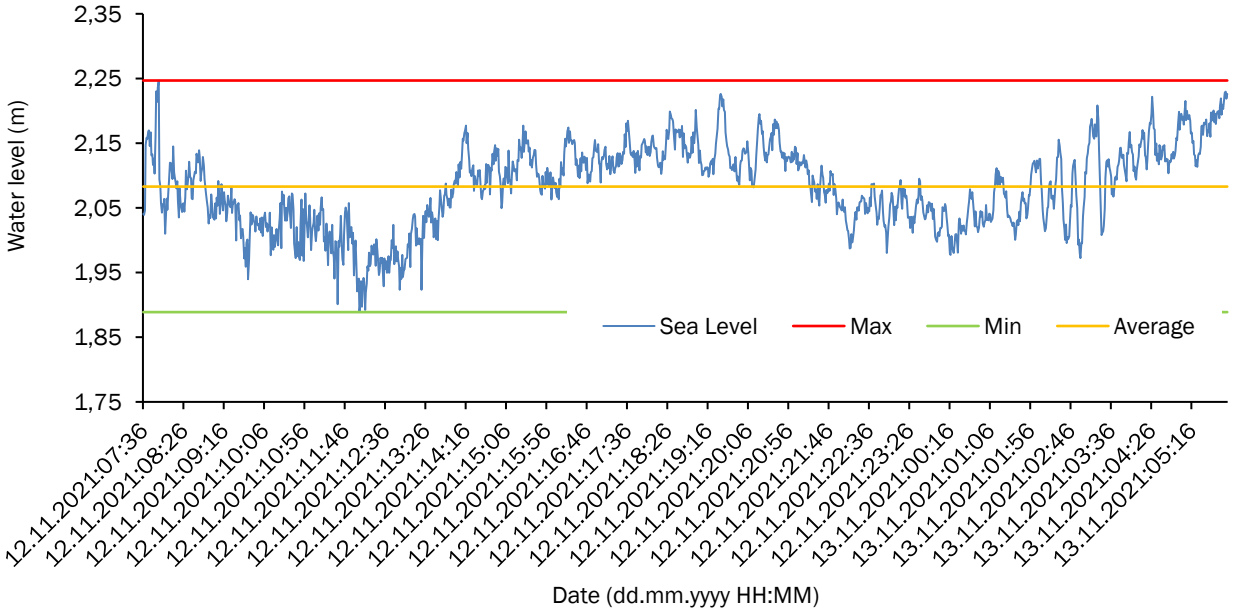

Figure 11. Results of air pressure to altitude conversion

R^2 value of 0.00931 shows a very low correlation between these two variables. This low correlation is likely due to wind, waves, and passing ships that can affect the air pressure readings and introduce noise into the measurements. The results of this study suggest that the BMP280 sensor is unsuitable for providing accurate sea level height measurements.

Tidal pattern based on air pressure

Based on the observations of air pressure measurements for one day, it was found that the measurements formed a sinusoidal pattern similar to the tidal pattern (Figure 13). The results of the tidal pattern, obtained from 23 hours of measurement, showed two highs and two lows with different amplitudes. The first high tide occurred at 09:47 with an air pressure value of 99,239.9 Pa and then receded at 15:28 with an air pressure value of 98,825.53 Pa. The second high tide occurred at 22:00 with an air pressure value of 99,194.27 Pa and the low tide at 03:00 with an air pressure value of 98,909.35 Pa. From these measurements, it can be inferred that the type of tide at Tanjung Siambang is a mixed tide.

Fourier analysis

The results of the Fourier analysis show that there are 6 constituent periods in air pressure measurements with the symbols S1, O2, M2, S2, S4, and S6 with periods of 24, 12.91, 12.42, 12, 6, and 4 h. Of the 6 components obtained, there are 2 main tidal components S2 and M2 with a period of 12 and 12.42 h. Based on the results of the Fourier analysis shown in Figure 14, it can be seen that the tide at

Tanjung Siambang is influenced by several factors, including the gravitational pull of the moon and the earth.

The M2 and S2 components are the dominant components, with periods of 12.42 and 12 h, respectively. The amplitude of these components is also relatively high, indicating that they have a significant impact on the tide patterns in the area. The results of this analysis can be used to better understand and predict tidal patterns in the future. Overall, the results of the Fourier analysis support the conclusion that the tide in Tanjung Siambang is a mixed tide.

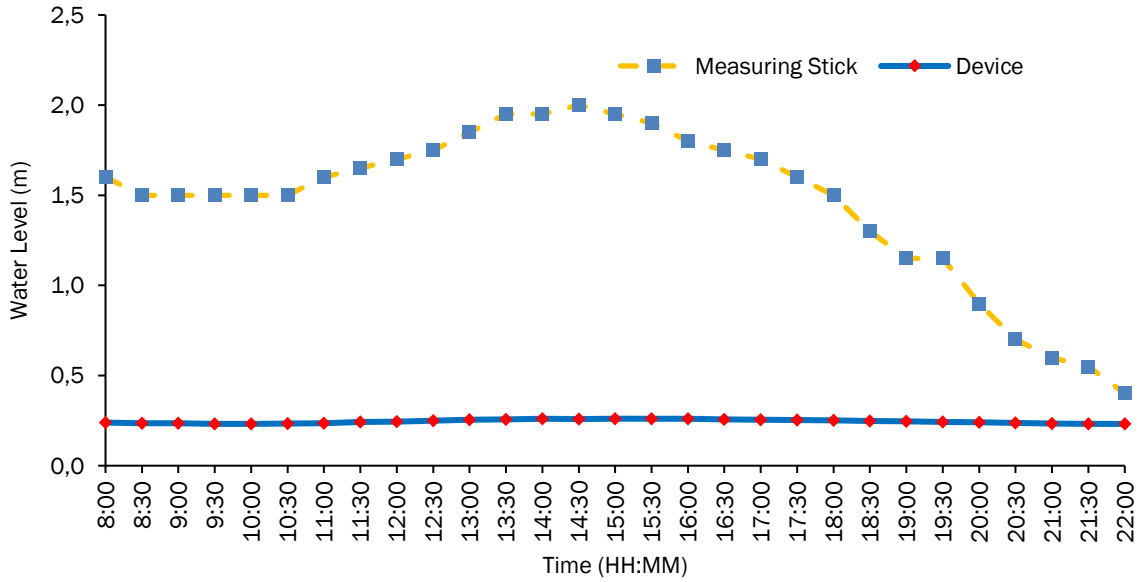

Figure 12. Water level comparison between device and measuring stick

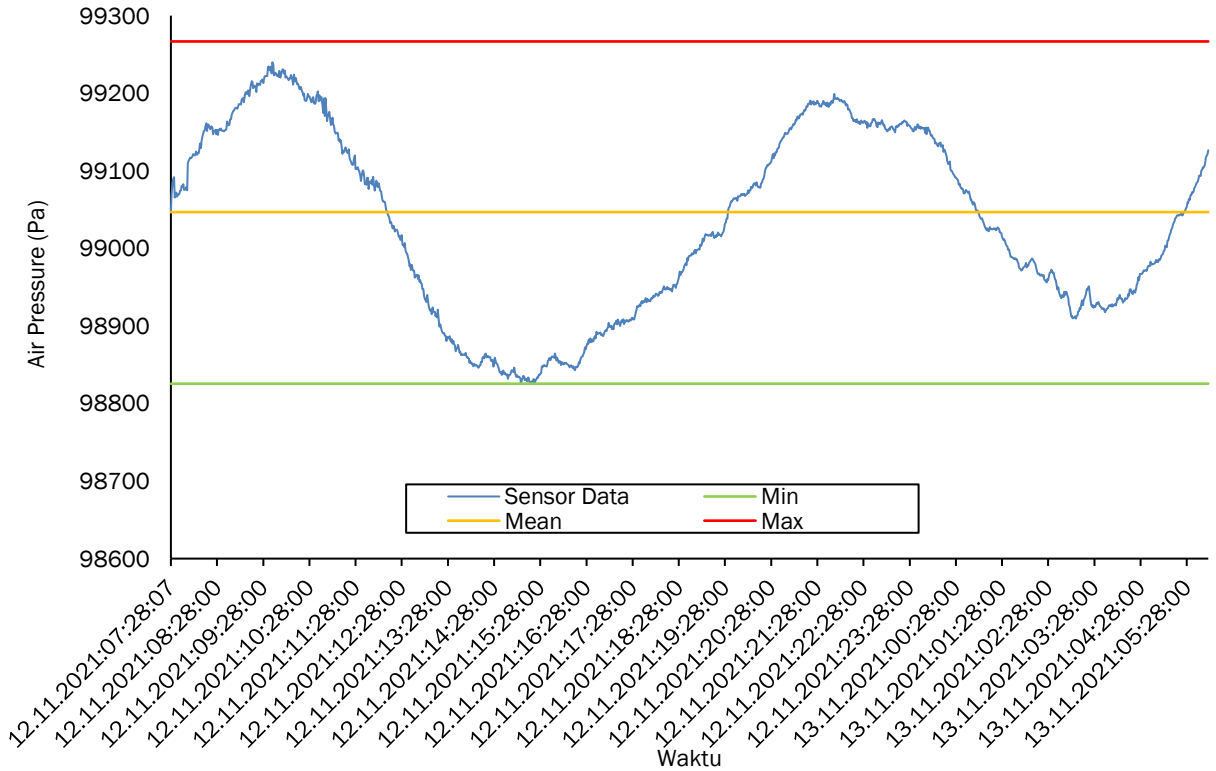

Figure 13. Tidal pattern based on air pressure measurement

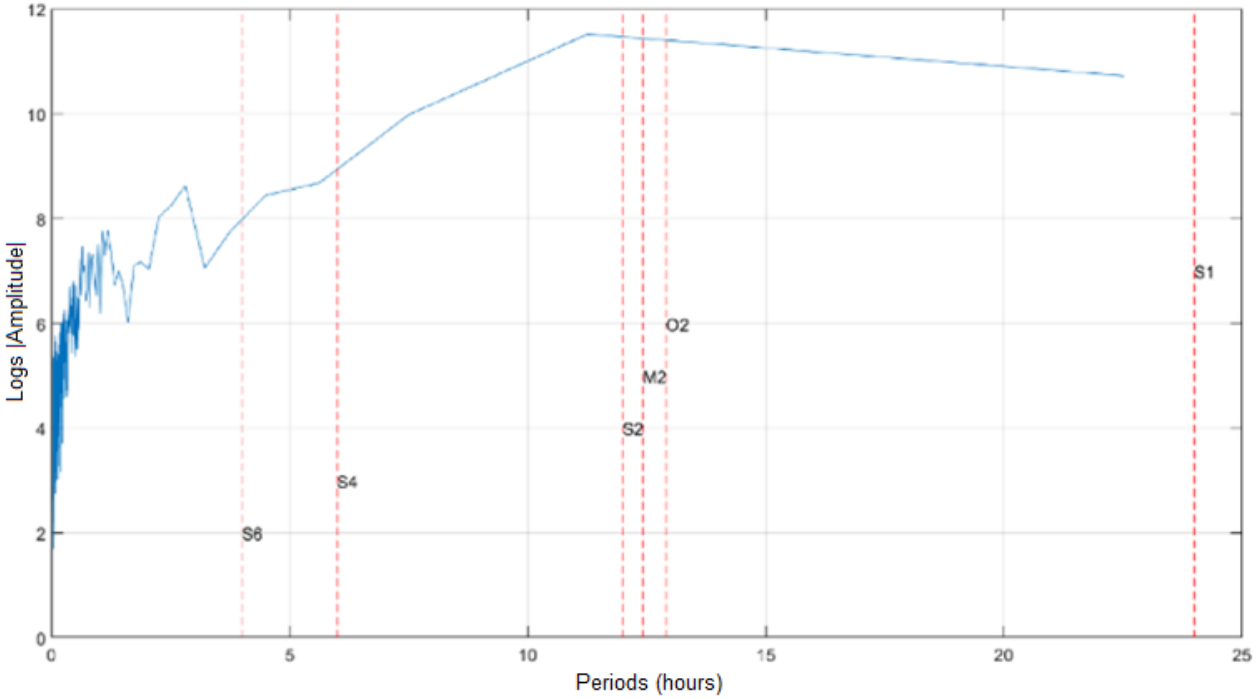

Figure 14. Fourier analysis results and tidal constituents

Tide gauges have been developed, such as acoustics, radar, and tide boards (Intergovernmental Oceanographic Commission, 2006; Irawan *et al.*, 2018). The air pressure characteristics can be used for tidal gauge applications. The higher the area above sea level, the air pressure will decrease (Yulkifli *et al*., 2014). Air pressure affects temperature. The higher the temperature, the air pressure will decrease (Giancoli, 2001; Fadholi, 2013).

The Bosch sensor is one of the air pressure gauge sensors (Bosch Sensortec, 2015). The BMP280 sensor is one of the Bosch sensors that researchers have widely used to measure air pressure (Budihartono *et al.*, 2020; Juwita and Suryadhi, 2018; Khaery *et al.*, 2020). In addition, several studies have successfully converted air pressure into altitude (Xia *et al*., 2015; Budihartono *et al*., 2020).

Based on the research results, the BMP280 sensor is more accurate than the BME280 sensor when measuring air pressure, which shows that the BMP280 is closer to the BMKG sensor than the BME280. Additionally, the linear regression measurement results show that the coefficient of determination for the BMP280 sensor is higher than the coefficient of determination for the BME280. The error rate for the BMP280 sensor is also lower at 0.16 hPa compared to the error rate for the BME280 sensor at 2.25 hPa. This result indicates that BMP280, as a low-cost sensor, offers many advantages for the efficient implementation of different applications (Ganev *et al.,* 2020), such as elevator velocity and weather station (Indrabayu *et al*., 2020; Nikolov *et al.*, 2020).

However, the BMP280 sensor cannot provide an accurate sea level height value when converting the air pressure data to altitude. Comparing the results of the air pressure conversion to altitude with gauges showed a low association between the two variables, with an R-squared value of 0.00931. This low association is likely due to several factors that affect the air pressure value, such as wind and waves, electrical noise, motion, weather, and climate (Xia *et al*., 2015; (Manivannan *et al.*, 2020).

Additionally, these research results indicated that the air pressure measurements formed a sinusoidal pattern similar to the tidal pattern, with two highs and two lows over 23 h. The Fourier analysis using FFT revealed six tidal components, with the main components being M2 and S2, caused by the moon's and the earth's gravitational pull. These two components are the most influential on the sea tides in Tanjung Siambang.

Based on Fourier analysis, tidal components composed periods with symbols S1, O2, M2, S2, S4, and S6 with periods of 24, 12.91, 12.42, 12, 6, and 4 h are the estimators that the type of tide in Tanjung

Siambang is mixed tide. This result also follows previous research, which said that the type of tides in the waters of Bintan Island is Mixed Semidiurnal Tide (Khairunnisa *et al.*, 2021). Additionally, M2 and S2 are dominant components that affect the tidal components (Kusuma *et al*., 2021).

The research suggests that the BMP280 sensor is reliable for measuring air pressure. However, it may not be suitable for determining sea level height in areas affected by various environmental factors. Further research may be needed to improve the accuracy of the BMP280 sensor in such environments.

Conclusion

This research has successfully designed and developed an instrument for measuring tides using a Bosch pressure sensor. The BMP280 sensor is more accurate than the BME280 sensor for measuring air pressure. The BMP280 sensor has a coefficient of determination of 0.9934 and an error rate of 0.16 hPa, while the BME280 sensor has a coefficient of determination of 0.9946 and an error rate of 2.25 hPa. Calibration is mandatory to decrease error. One-way ANOVA proves that pressure sensors statistically do not differ from the BMKG sensor after the calibration. However, the BMP280 sensor cannot provide accurate results when measuring sea level height. Various factors, such as wind, waves, weather, climate, and electronic noise, can affect the air pressure value and introduce noise into the measurements. Additionally, it was found that air pressure measurements in Tanjung Siambang exhibit a sinusoidal pattern similar to the tidal pattern and that the tide in Tanjung Siambang is mixed based on Fourier analysis. The main tidal components found were M2 and S2, caused by the moon's and the earth's gravitational pull.

Acknowledgement

This research has been supported by Department of Electrical Engineering Universitas Maritim Raja Ali Haji. Asri Dinata, Parasian Sihombing, and M. Hafiz Alfahmi for helping the field test.

References

Albaladejo-Perez, C., Soto Valles, F., Torres Sanchez, R., Jimenez Buendia, M., Lopez-Castejon, F. & Gilabert Cervera, J. 2017. Design and Deployment of a Wireless Sensor Network for the Mar Menor Coastal Observation System. *IEEE J. Oceanic Eng.*, 42(4): 966–976. https://doi.org/10.1109/JOE.2016.2639118

Asaad, I., Lundquist, C.J., Erdmann, M.V & Costello, M.J. 2018. Delineating priority areas for marine biodiversity conservation in the Coral Triangle. *Biolog. Conserv.*, 222: 198–211. https://doi.org/10.1016/j.biocon.2018.03.037

Bello, O. & Zeadally, S. 2022. Internet of underwater things communication: Architecture, technolo - gies, research challenges and future opportunities. *Ad Hoc Networks*, 135: p.102933 https://doi.org/10.1016/j.adhoc.2022.102933

Bolanakis, D.E. 2017. Evaluating performance of MEMS barometric sensors in differential altimetry systems. *IEEE Aerosp. Electron. Syst. Mag.*, 32(9): 34–39. https://doi.org/10.1109/MAES.2017.160248

Bolanakis, D.E., Kotsis, K.T. & Laopoulos, T. 2015. A prototype wireless sensor network system for a comparative evaluation of differential and absolute barometric altimetry. *IEEE Aerosp. Electron. Syst. Mag.,* 30(11): 20–28. https://doi.org/10.1109/MAES.2015.150013

Bosch Sensortec. 2015. *BMP280: Datasheet*. Retrieved from https://cdn-shop.adafruit.com/datasheets/BST-BMP280-DS001-11.pdf

Budihartono, E., Afriliana, I. & Rakhman, A. 2020. Analisa Penggunaan Alat Pengukur Ketinggian Menggunakan. *Smart Comp.*, 9(1): 31–34. https://doi.org/10.30591/smartcomp.v9i1.18 16

Dickow, A. & Feiertag, G. 2014. A framework for calibration of barometric MEMS pressure sensors. *Procedia Eng.*, 87: 1350–1353. https://doi.org/10.1016/j.proeng.2014.11.716

Dina, A., Atmodjo, W. & Setiyo Pranowo, W. 2019. Karakteristik Pasang Surut di Teluk Jakarta Berdasarkan Data 253 Bulan. *J. Riset Jakarta*, 12(1): 25–36. https://doi.org/10.37439/jurnaldrd.v12i1.7

Fadholi, A. 2013. Study Pengaruh Suhu Dan Tekanan Udara Terhadap Operasi Penerbangan Di Bandara H.A.S. Hananjoeddin Buluh Tumbang Belitung Periode 1980-2010. *J. Penelitian Fisika Dan Aplikasinya*, 3(1): 1-10. https://doi.org/10.26740/jpfa.v3n1.p1-10

Fadly, R. & Dewi, Ci. 2019. Pengembangan Sensor Ultrasoic Guna Pengukuran Pasang Surut Laut Secara Otomatis dan Real Time. *J. Rekayasa*, 23(1): 1–16.

Ganev, B., Nikolov, D. & Marinov, M.B. 2020. Performance evaluation of MEMS pressure

sensors. *11th National Conf. Int. Participation, Electronica 2020 - Proceedings*, p.23–26. https://doi.org/10.1109/ELECTRONICA50406.2020.9305140

Giancoli, D.C. 2001. Fisika 1 (fifth). Jakarta: Erlangga.

Guo, Y., Han, Q. & Kang, X. 2020. Underwater sensor networks localization based on mobility-constrained beacon. *Wirel. Netw.*, 26(4): 2585–2594. https://doi.org/10.1007/s11276-019-02023-5

Haq, M. R. & Ni, Z. 2019. A new hybrid model for short-term electricity load forecasting. *IEEE Access*, 7: p.125413–125423. https://doi.org/10.1109/ACCESS.2019.2937222

Haq, N.A., Khomsin & Pratomo, D.G. 2021. The Design of an Arduino Based Low-Cost Ultrasonic Tide Gauge with the Internet of Things (IoT) System. *IOP Conf. Ser. Earth Environ. Sci.*, 698(1): p.012004 https://doi.org/10.1088/1755-1315/698/1/012004

Hossain, D., Imtiaz, M.H. & Sazonov, E. 2020. Comparison of Wearable Sensors for Estimation of Chewing Strength. *IEEE Sens. J.*, 20(10): 5379–5388. https://doi.org/10.1109/JSEN.2020.2968009

Indrabayu, Pallu, S., Achmad, A., Areni, I. S. & Bustamin, A. 2020. A prototype of low cost weather station for data spatial and temporal analysis. *ICIC Express Letters*, 14(11): 1121–1127. https://doi.org/10.24507/icicel.14.11.1121

Intergovernmental Oceanographic Commission. 2006. Manual on Sea Level Measurement and Interpretation, Volume IV: An Update to 2006. IOC Manuals and Guides No.14, Vol. IV ; JCOMM Technical Report No. 31.

Irawan, S., Fahmi, R. & Roziqin, A. 2018. Kondisi Hidro Oseanografi (Pasang Surut, Arus Laut, Dan Gelombang) Perairan Nongsa Batam. *J. Kel.: Indonesian J. Mar. Sci. Technol.,*11(1): 56-68. https://doi.org/ 10.21107/jk.v11i1.4496

Irtawaty, A.S. 2019. Implementasi Metode Fast Fourier Transform (FFT) Dalam Mengklasifikasikan Suara Pria Dan Wanita Di Laboratorium Jurusan Teknik Elektro Politeknik Negeri Balikpapan. *J. Teknologi Terpadu*, 7(2): 70–75. https://doi.org/10.32487/jtt.v7 i2.661

Juwita, L.E. & Suryadhi, S. 2018. Rancang Bangun Sistem Observasi Keadaan Atmosfer Bumi Menggunakan Drone. *J. Electrical and Electronic Engineering-UMSIDA*, 2(2): 86–91. https://doi.org/10.21070/jeee-u.v2i2.1700

Khaery, M., Pratama, A.H., Wipradnyana, P. & Gunawan, A.A.N. 2020. Design of Air Pressure Measuring Devices Using a Barometric Pressure 280 (BMP280) Sensor Based on Arduino Uno. *Buletin Fisika*, 21(1): p.14. https://doi.org/10.24843/bf.2020.v21.i01.p03

Khairunnisa, K., Apdillah, D. & Putra, R.D. 2021. Karakteristik Pasang Surut Di Perairan Pulau Bintan Bagian Timur Menggunakan Metode Admiralty. *J. Kel.: Indonesian J. Mar. Scie. Technol.* 14(1): 58–69. https://doi.org/10.21107 /jk.v14i1.9928

Kumar, S. & Tanwar, A. 2020. Development of a MEMS-based barometric pressure sensor for micro air vehicle (MAV) altitude measurement. *Microsyst. Technolog.*, 26(3): 901–912. https://doi.org/10.1007/s00542-019-04594-x

Kusuma, H.A., Lubis, M.Z., Oktaviani, N. & Setyono, D.E.D. 2021. Tides Measurement and Tidal Analysis at Jakarta Bay. *J. Applied Geospatial Information*, 5(2): 494–501. https://doi.org/10.30871/jagi.v5i2.2779

Manivannan, A., Chin, W.C.B., Barrat, A. & Bouffanais, R. 2020. On the challenges and potential of using barometric sensors to track human activity. *Sensors,* 20(23): 1–36. https://doi.org/10.3390/s20236786

Mendenhall, W., Beaver, R.J. & Beaver, B.M. (2013). Introduction to Probability and Statistics. (M. Julet,Ed.) (14th ed.). Boston: Brooks/Cole.

Missa, I.K., Lapono, L.A.S. & Wahid, A. 2018. Rancang Bangun Alat Pasang Surut Air Laut Berbasis Arduino Uno Dengan Menggunakan Sensor Ultrasonik Hc-Sr04. *J.Fisika : Fisika Sains Dan Aplikasinya*, 3(2): 102–105. https://doi.org/10.35508/fisa.v3i2.609

Nikolov, D.N., Marinov, M.B., Ganev, B.T. & Djamijkov, T.S. 2020. Nonintrusive Measurement of Elevator Velocity Based on Inertial and Barometric Sensors in Autonomous Node. *2020 43rd Int.Spring Seminar on Electronics Technol.,* pp. 1–5. https://doi.org/10.1109/ISSE49702.2020.9121077

Nugent, C. 2019. Fundamentals of Clinical Data Science. (P. Kubben, M. Dumontier & A. Dekker,Eds.), The Routledge Companion to Media and Fairy-Tale Cultures. Cham: Springer International Publishing. https://doi.org/10.1007/978-3-319-99713-1

Qiang, L., Bing-Dong, Y. & Bi-Guang, H. 2018. Calculation and Measurement of Tide Height for the Navigation of Ship at High Tide Using Artificial Neural Network. *Polish Maritime Research*, 25(s3): 99–110. https://doi.org/10.2478/pomr-2018-0118

Richter, A.J., Marderwald, E.R., Hormaechea, J.L., Mendoza, L.P.O., Perdomo, R.A., Connon, G.C., Scheinert, M., Horwath, M. & Dietrich, R. 2016. Lake-level variations and tides in Lago Argentino, Patagonia: Insights from pressure tide gauge records. *J. Limnolog.*, 75(1): 62–77. https://doi.org/10.4081/jlimnol.2015.1189

Rudiastuti, A.W., Syafi'i, A.N. and Kusuma, H.A., 2019, December. Spatial pattern of tides in Indonesia using altimetry data. *Sixth International Symposium on LAPAN-IPB Satellite,* 11372: 529-535. https://doi.org/10.1117/12.2542855

Tirtasari, N.L., 2017. Uji Kalibrasi (Ketidakpastian Pengukuran) Neraca Analitik Di Laboratorium Biologi Fmipa Unnes. *Indones. J. Chem. Sci.*, 6(2): 151–155.

Towler, R. & Williams, K. 2010. An inexpensive millimeter-accuracy electronic length measuring board. *Fish. Res.*, 106(1): 107–111. https://doi.org/10.1016/j.fishres. 2010. 06. 012

Wang, R.Q., Stacey, M.T., Herdman, L.M.M., Barnard, P.L. & Erikson, L. 2018. The Influence of Sea Level Rise on the Regional Interdependence of Coastal Infrastructure. *Earth's Future*, 6(5): 677–688. https://doi.org/10.1002/2017EF000742

Xia, H., Wang, X., Qiao, Y., Jian, J. & Chang, Y. 2015. Using Multiple Barometers to Detect the Floor Location of Smart Phones with Built-in Barometric Sensors for Indoor Positioning. *Sensors*, 15(4): 7857–7877. https://doi.org/10.3390/s150407857

Yulkifli, Asrizal & Ardi, R. 2014. Pengukuran Tekanan Udara Menggunakan Dt-Sense Barometric Presure Berbasis Sensor Hp03. *J. Sainstek IAIN Batusangkar*, 6(2): 110–115. https://doi.org/10.31958/js.v6i2.110

Appendix 1. Comparison measurement differences between BMKG, BMP280, and BME280 sensors in calibration

NO	BMKG Sensor (hPa)	Sensor calibration (hPa)				Measurement difference (hPa)			
		Before		After		Before		After	
		BMP280	BME280	BMP280	BME280	BMP280	BME280	BMP280	BME280
	D1	D2	D3	D4	D5	D2-D1	D3-D1	D4-D1	D5-D1
1	1011.6	1011.3	1009.3	1011.68	1013.58	-0.30	-2.30	0.08	1.98
2	1011.6	1011.3	1009.2	1011.68	1013.58	-0.30	-2.40	0.08	1.98
...	...	...	...	...	...	...	...	...	...
101	1010.5	1010.1	1008.1	1010.59	1012.38	-1.50	-3.50	-1.01	0.78
102	1010.5	1010.2	1008.1	1010.59	1012.48	-1.40	-3.50	-1.01	0.88
...	...	...	...	...	...	...	...	...	...
201	1009.8	1009.7	1007.5	1009.90	1011.98	-1.90	-4.10	-1.70	0.38
202	1009.8	1009.7	1007.5	1009.90	1011.98	-1.90	-4.10	-1.70	0.38
...	...	...	...	...	...	...	...	...	...
301	1009.1	1009	1007	1009.21	1011.28	-2.60	-4.60	-2.39	-0.32
302	1009.1	1009	1006.9	1009.21	1011.28	-2.60	-4.70	-2.39	-0.32
...	...	...	...	...	...	...	...	...	...
401	1008.6	1008.6	1006.5	1008.71	1010.88	-3.00	-5.10	-2.89	-0.72
402	1008.6	1008.5	1006.5	1008.71	1010.78	-3.10	-5.10	-2.89	-0.82
...	...	...	...	...	...	...	...	...	...
501	1010.1	1009.9	1007.8	1010.20	1012.18	-1.70	-3.80	-1.40	0.58
502	1010.1	1009.9	1007.8	1010.20	1012.18	-1.70	-3.80	-1.40	0.58
...	...	...	...	...	...	...	...	...	...
601	1010.9	1010.8	1008.7	1010.99	1013.08	-0.80	-2.90	-0.61	1.48
602	1010.9	1010.8	1008.7	1010.99	1013.08	-0.80	-2.90	-0.61	1.48
...	...	...	...	...	...	...	...	...	...
701	1011.7	1011.6	1009.5	1011.78	1013.88	0.00	-2.10	0.18	2.28
702	1011.7	1011.5	1009.4	1011.78	1013.78	-0.10	-2.20	0.18	2.18
...	...	...	...	...	...	...	...	...	...
801	1011.6	1011.4	1009.3	1011.68	1013.68	-0.20	-2.30	0.08	2.08
802	1011.6	1011.4	1009.3	1011.68	1013.68	-0.20	-2.30	0.08	2.08
...	...	...	...	...	...	...	...	...	...
901	1010.2	1010.1	1007.9	1010.30	1012.38	-1.50	-3.70	-1.30	0.78
902	1010.2	1010	1007.9	1010.30	1012.28	-1.60	-3.70	-1.30	0.68
...	...	...	...	...	...	...	...	...	...
1001	1009.1	1009	1006.8	1009.21	1011.28	-2.60	-4.80	-2.39	-0.32
1002	1009.1	1008.9	1006.9	1009.21	1011.18	-2.70	-4.70	-2.39	-0.42
...	...	...	...	...	...	...	...	...	...
1101	1009.3	1009.2	1007.1	1009.41	1011.48	-2.40	-4.50	-2.19	-0.12
1102	1009.3	1009.2	1007.1	1009.41	1011.48	-2.40	-4.50	-2.19	-0.12
...	...	...	...	...	...	...	...	...	...
1201	1010.3	1010.3	1008.1	1010.39	1012.58	-1.30	-3.50	-1.21	0.98
1202	1010.3	1010.3	1008.1	1010.39	1012.58	-1.30	-3.50	-1.21	0.98
...	...	...	...	...	...	...	...	...	...
1301	1011.5	1011.4	1009.3	1011.58	1013.68	-0.20	-2.30	-0.02	2.08
1302	1011.4	1011.4	1009.3	1011.48	1013.68	-0.20	-2.30	-0.12	2.08
...	...	...	...	...	...	...	...	...	...
1401	1011.7	1011.7	1009.6	1011.78	1013.98	0.10	-2.00	0.18	2.38
1402	1011.7	1011.7	1009.6	1011.78	1013.98	0.10	-2.00	0.18	2.38
...	...	...	...	...	...	...	...	...	...
1440	1011.9	1011.8	1009.7	1011.98	1014.08	0.20	-1.90	0.38	2.48
1441	1011.9	1011.8	1009.7	1011.98	1014.08	0.20	-1.90	0.38	2.48
...	...	...	...	...	...	...	...	...	...
1450	1011.8	1011.7	1009.6	1011.88	1013.98	0.10	-2.00	0.28	2.38
1451	1011.8	1011.7	1009.6	1011.88	1013.98	0.10	-2.00	0.28	2.38
...	...	...	...	...	...	...	...	...	...
1463	1011.7	1011.5	1009.4	1011.78	1013.78	-0.10	-2.20	0.18	2.18
1464	1011.6	1011.5	1009.4	1011.68	1013.78	-0.10	-2.20	0.08	2.18